The Influence of Thermal and Mechanical Effects on the Bond Formation During Impact Welding

C. Pabst*, P. Groche

Institute for Production Engineering and Forming Machines, TU Darmstadt, Germany
*Corresponding author. Email: pabst@ptu.tu-darmstadt.de

Abstract

Impact welding, usually applied as explosion welding or electromagnetic pulse welding, is a highly transient joining process. Strain rates in orders of magnitude far above 10^4 1/s and resultant thermal effects occur and influence the formation of the joint significantly. Experimental and microscopic investigations as well as analytical estimations are carried out and presented in this paper in order to gain a more comprehensive understanding of the effective mechanisms and their relevance. In addition to electromagnetic pulse welding, a specially built test rig is used to identify the process window and its change due to modified parameters. The test rig allows to change both impact parameters, angle β and velocity v_c, independently.

It will be shown that the actual formation of the joint and its characteristics are greatly affected by the surrounding gaseous media. Strength and size of the joint can be influenced as well as the location of the process window. Theories will be developed to explain these results and to make them usable for the practical application. Furthermore, experimental results indicate that the compression of the ambient atmosphere in the closing gap between the two specimens evokes highly elevated temperature, which is in good accordance with earlier findings.

Keywords

Joining, Impact welding, Bond formation

1 Introduction

The discovery of impact welding is traced back to the First World War, when it was found accidentally that shrapnel sometimes stuck to armour (Crossland, 1982). The first industrial application to be developed in the following years was explosion welding (Carl, 1944). The blast wave of an explosive accelerates a metal sheet (the so-called flyer) up to several hundred meters per second towards a second metal sheet (the so-called target). The metallurgical joint is formed during the impact and does not require melting (Crossland, 1982). This is why impact welding even allows joints between dissimilar metals (Crossland, 1982).

Later, electromagnetic pulse welding has been developed. The force from the blast wave is replaced by electromagnetic forces which are evoked by a strong, pulsed current in a tool coil. The process principles are identical to explosion welding. However, the capacitors of a typical pulse generator deliver a much lower amount of energy than the explosives. This leads to potentially smaller weld areas and smaller material thicknesses for the flyer in electromagnetic pulse welding. This drawback is compensated by the fact that electromagnetic pulse welding is safe and suitable for mass production with cycle times in the range of only few seconds. (Schäfer et al., 2011)

Both processes have in common that the parts to be joined can have almost any shape. Formed sheets as well as tubular structures are possible. Both processes also share the same impact principle. The geometry as well as the force distribution have to be designed in a way that there is a specific angle between the parts during the impact. This leads to a collision line (or collision point in a cross section) travelling across the surface. The normal impact velocity is, as already mentioned, in the range of some hundred meters per second. The angle is usually in the range between 5° and 35°. The velocity of the collision point is in the range of several thousand metres per second and thus always supersonic. The process window for each material combination which has been developed for explosion welding is usually given dependent on the angle and the velocity of the collision point. (Crossland, 1982)

In order to establish a sound weld, a characteristic phenomenon is important: The so-called jetting process (Crossland, 1982). Due to the hydrodynamic flow of material at strain rates far above 10^4 1/s (Crossland, 1982) directly at the impact area, superficial layers of both parts are ejected from the closing gap. In earlier scientific investigations the presence of this jet has been proven by high speed imaging, numerical analyses (Wang et al., 2012) and catching the ejected material (Bergmann et al., 1966). A range of experiments has been conducted: The impact has been generated for example by the use of a gun (Turgutlu et al. 1995) or electromagnetic pulse technology (Kakizaki et al. 2011).

The aim of the studies presented in this paper is to provide additional knowledge on the process mechanisms. Currently, the design of impact welding joints is often done empirically and thus is very time consuming. Additionally, a targeted process optimisation and the prediction of the actual weld strength are almost impossible.

2 Experimental Setups

For the conducted experiments within this paper, two techniques are utilized: electromagnetic pulse welding and a specially designed test rig.

2.1 Electromagnetic Pulse Welding

A pulse generator and a tool coil are the core components of a system for electromagnetic pulse welding. The pulse generator mainly consists of large capacitors which are charged with voltages of several kilovolts. Special switches connect the capacitors to the tool coil and form an oscillating circuit. The damped current reaches several hundred kiloamperes at frequencies mainly in the range between 10 kHz and 50 kHz. The experiments presented in this paper are carried out with a sheet welding coil. The effective part of the coil with a cross section of 5 mm x 5 mm and the position of the sheets to be welded are shown in **Fig. 1**. The distance between the coil and the flyer sheet 0.5 mm, which is determined by an insulation sheet.

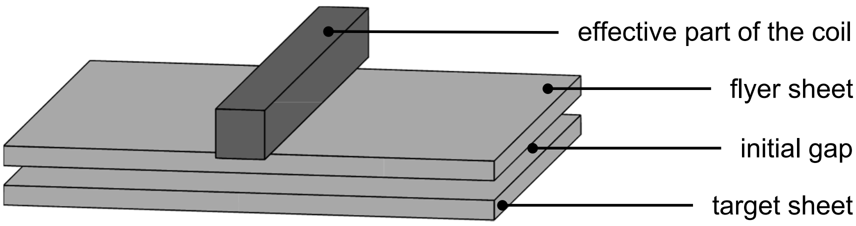

Figure 1*: Sketch of the electromagnetic pulse welding setup*

A photo of a welded specimen is depicted in **Fig. 2**. Only the material close to the coil is moved due to the spacers and the inertia.

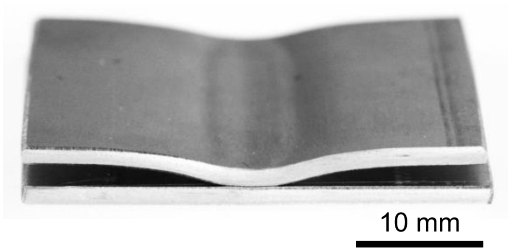

Figure 2*: Welded specimen*

2.2 Test Rig

For basic research, electromagnetic pulse welding exhibits the disadvantage of being transient. This means that the angle at the collision point and its velocity constantly change during the impact (Groche et al., 2014). To overcome this limitation, a special test rig has been developed which is shown in **Fig. 3**. It is capable of colliding specimens at constant and well defined angles and velocities. Each of the two specimens is attached to one aluminium rotor with a diameter of 500 mm. The impact takes place when the acceleration up to 5000 rpm is finished after about 1.5 s. This equals 131 m/s for each specimen and a relative velocity of 262 m/s.

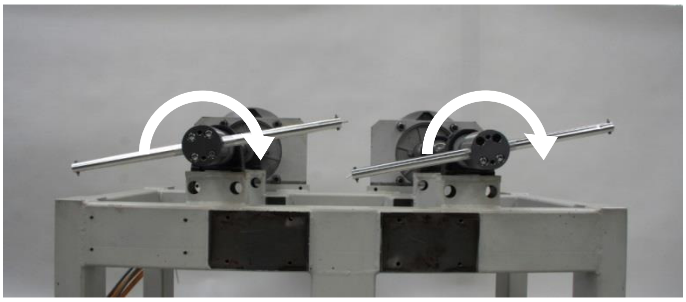

***Figure 3**: Test rig (without housing): Two motors drive one rotor each with one specimen attached at one end*

The impact velocity is directly adjusted by the number of revolutions per minute and the angle is determined by bending one specimen accordingly. After the collision the welded parts of the specimens are torn off at a breaking point, whereas the rest stays attached to the rotors. **Fig. 4** shows the adjusted angle between the specimens (a) and a welded specimen (b) with the end remaining attached to the rotors after the collision.

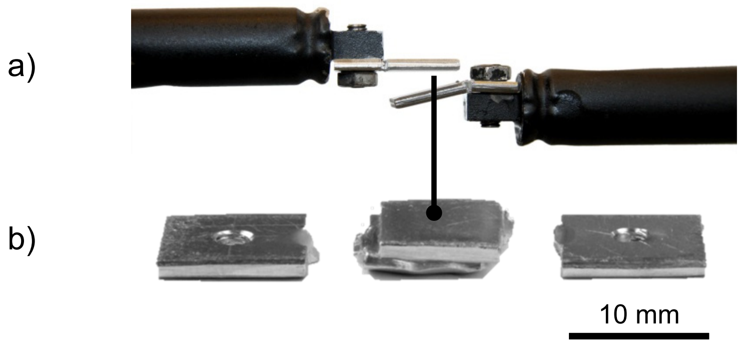

***Figure 4**: Adjustment of the impact angle by bending one specimen (a) and welded sample (b)*

The collision point velocity can be directly calculated from the geometrical relationship between impact velocity and impact angle. Furthermore, these parameters remain constant during the impact. The comparability between electromagnetic pulse welding and the developed test rig has been shown in earlier works by experimental investigations (Groche et al. 2014) and numerical studies (Groche and Pabst, 2015).

3 The Influence of the Surrounding Medium During Welding

Investigations in earlier publications have shown that the surrounding gaseous medium has an effect on the process. In (Groche and Pabst, 2014), an effect could be observed when replacing the ambient air by argon. Bergmann et al. (1966) investigated explosion welding of two aluminium sheets in an atmospheric atmosphere and in a vacuum chamber. The alloy remains unspecified. With the help of high speed imaging they found that the velocity of the jet in vacuum is about twice as high as under atmospheric pressure. However, they did not observe any effect on the morphology of the weld in micrographs.

3.1 Experimental Setup

In order to investigate the effect of low air pressure, a similar experiment is carried out for electromagnetic pulse welding. The two sheets to be welded are made of commercially pure aluminium (99.5%, EN AW-1050A) in half hard condition (Hx4). The size is 40 mm x 40 mm x 2 mm and the initial distance was adjusted to 2 mm. The working frequency of the system is 19.6 kHz, the charging energy is varied to achieve different peak discharge currents and thus different impact velocities and energies. The peak current is varied between 250 kA, 260 kA, 288 kA and 313 kA. The two aluminium sheets on the coil are covered by an acrylic glass case which allows the process observation. The vacuum is created prior to the discharge and the pressure is approximately 100 mbar.

3.2 Process Observation

During the impact, a significant difference could be observed immediately between vacuum and atmospheric pressure: The typical flash during the impact between the two sheets became significantly darker in vacuum, which can be seen in the direct comparison in **Fig. 5**. The tool coil is located at the bottom under an electrical insulation sheet and the two sheet specimens are held down by a fixture from the top. The photos are taken by a conventional camera with a long exposure time to capture the complete process without the need of a trigger signal.

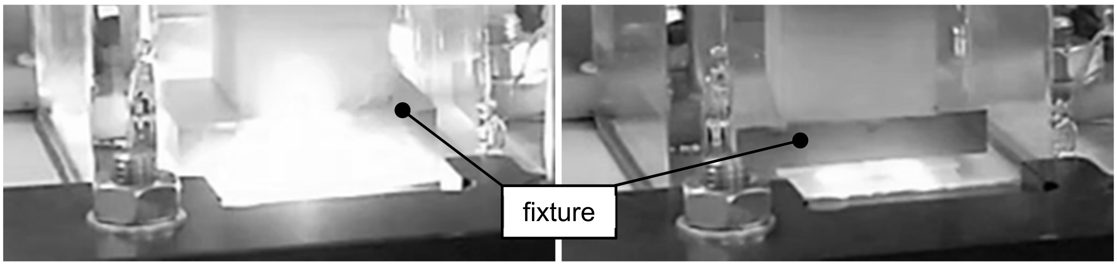

***Figure 5**: The process light at ambient pressure (left) and in vacuum (right).*

This observation is in accordance with former findings and supports an earlier theory on the formation of the light. The authors proposed that the light is caused by the supersonic compression of the surrounding medium, the ambient atmosphere in this case. The compression occurs very fast and is capable of evoking plasma (Koschlig et al., 2008). During the experiments with 250 kA, no light at all could be seen in vacuum, whereas it was still visible at normal pressure. It should be noted that no weld was possible with this current.

3.3 Macroscopical and Microscopical Investigation

Peel tests after the welding experiments with low currents (250 kA and 260 kA) showed that the size of the potentially joined area, which can be identified as white surfaces in **Fig. 6**, can be increased drastically in vacuum. This area exhibits the characteristic O-shape for electromagnetic pulse welding and this setup of the sheets and the coil (Schäfer et al., 2011). At higher currents these areas are welded and thus it was no more possible to damage the weld and estimate its size in the peel test, because the failure occurred in the parent material.

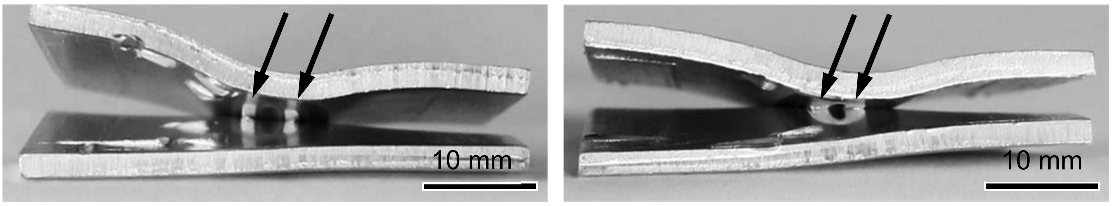

***Figure 6**: Result of the peel test for welded samples at ambient pressure (left) and in vacuum (right) at 260 kA.*

A weld is possible starting at a peak current of 288 kA. Two samples at ambient pressure and in vacuum were used for further, microscopic investigations. The macroscopic overview on the polished cross sections in **Fig. 7** gives a first idea of the size of the actual metallurgical joint.

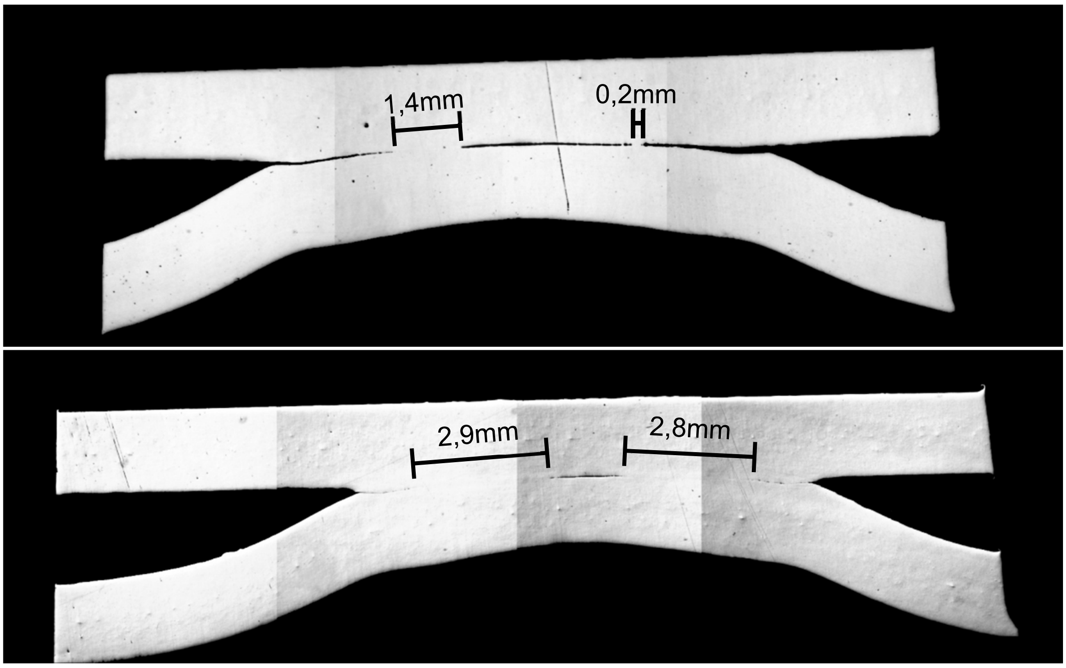

***Figure 7**: Cross section of the samples welded with a peak current of 288 kA at ambient pressure (top) and in vacuum (bottom).*

The total width of the weld is about 1.6 mm at ambient pressure, whereas it reaches about 5.7 mm in vacuum. The distribution of welded and unwelded areas is typical for this setup in electromagnetic pulse welding (Watanabe and Kumai, 2009). In the central area where the first contact occurs, no joint is possible because the impact angle is too small. The collision point then travels symmetrically to the left and the right. Its speed and the angle reach the process window shortly afterwards and a metallurgical joint is formed. Due to the limited size of the effective area of the tool coil and limited process energy in electromagnetic pulse welding compared to explosion welding, the kinetic energy is transformed steadily into forming energy. The decrease in velocity first stops the bond formation and finally stops the movement. Thus the weld area never spreads across the whole area where both sheets are in contact.

It could be suspected that the difference in the weld lengths is caused by the missing air that has to be pushed out of the continuously closing gap between the two sheets during the process. In this setup, the volume of ejected gas and moved aluminium at the same time is roughly the same. Taking into account that air at normal pressure is by the factor 2250 lighter than aluminium, it can be safely concluded that this effect may be present, but is not relevant. The comparison in **Fig. 8** of the final contours of the two specimens supports this consideration, as there is no clearly visible difference between them.

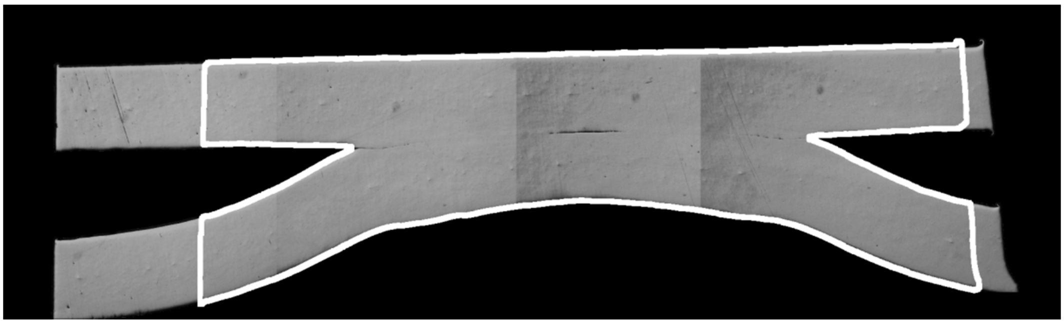

Figure 8: *Comparison between the vacuum sample and the ambient pressure sample (white contour)*

The micrographs, especially at the unwelded areas, show one main difference between the two samples. The gap in the unwelded areas is in the range of 17 µm up to 50 µm for the atmospheric pressure sample, whereas the vacuum sample exhibits gaps in the range of only 9 µm and below, **Fig. 9**. A closer look at the gaps in the atmospheric pressure sample shows numerous aluminium particles in various sizes from 3000 µm² down to only a few square micrometres. One of these particles is marked in **Fig. 9**. These cannot be observed in the vacuum sample.

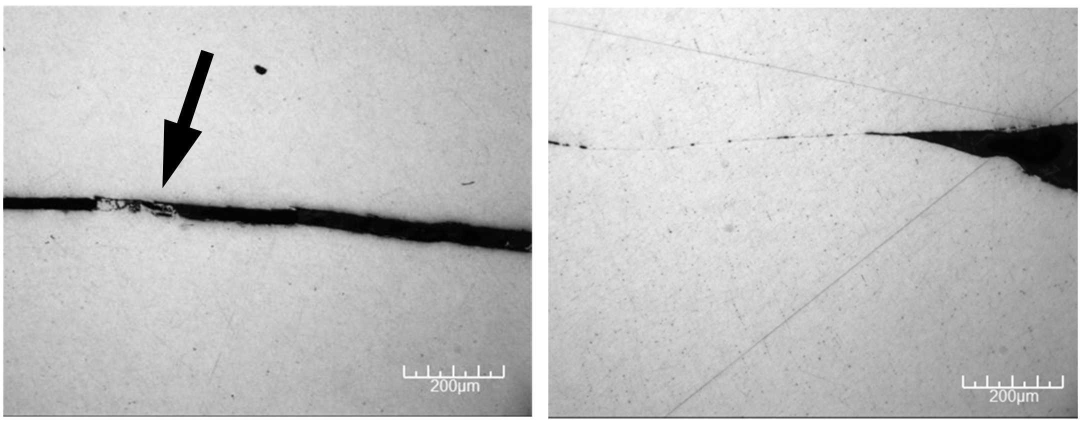

Figure 9: *The unwelded gap between the two sheets on the very right side of the cross section for the weld at ambient pressure (left) and in vacuum (right)*

3.4 Interpretation

It can be concluded that the so-called jet and the process light are two independent phenomena during impact welding. The experiments have shown that it is possible to reduce or even suppress the light but still obtain a weld. As a weld always requires the existence of the jet, it has still to be present. Immediately after the impact, it can be actually seen with the bare eye as a small amount of dust that is expelled from the joint area. Furthermore, the weld quality can be even increased drastically, at least at the lower end of the process window. The reason might be the missing or at least decreased air resistance for the jet, which allows the particles to escape much easier from the closing gap between the sheets. This theory is supported by the presence of aluminium particles between the sheets after the process at ambient pressure. They cannot be found in the specimens which have been welded in vacuum. The findings of Bergmann et al. (1966) about the increased velocity of the jet in vacuum also support this theory. Additionally, their investigations suggest that this effect does not influence the weld quality any more at higher impact energies. A possible explanation is that the jet too has a higher kinetic energy and thus can escape from the gap completely despite the air resistance.

4 Estimation of the Temperature in the Weld Area

Impact welded joints, especially at higher energies, often show areas of presumably molten material between dissimilar metals (Göbel et al., 2010) and also similar metals (Stern et al., 2014). One reason is the high strain rate in the impact area. In earlier publications the authors of this paper suggested that the supersonic compression of the surrounding gas is fast enough to also cause extremely high temperatures far above 1000 K and thus create plasma (Groche and Pabst, 2014). This was supported by former analytical investigations on the temperature rise due to the compression of different gases by Koschlig et al. (2008). The experimental verification of this theory is possible but challenging due to the small dimensions and the short duration of the impact process in the range of microseconds. In order to gain first information on the temperatures during the impact ozone measurement is applied. Ozone is sensitive to an increase in temperature. According to Clement (1904), more ozone is generated at higher temperatures, but the decay increases more rapidly. If a significant increase in temperature occurs, this should be detectable by a decrease of the ozone concentration. The experiments are carried out at the developed test rig due to its good accessibility. Furthermore, unwanted effects due to sparkovers between the two sheets in electromagnetic pulse welding are avoided.

4.1 Measurement Technique

The air is directly taken from the location where the two specimens collide via a short hose, **Fig. 10**. The ozone measurement device is specially developed for fast data acquisition rates of up to 50 Hz whereas conventional instruments are usually limited to about 2 Hz. However, the device is not capable of providing absolute values of the ozone concentration. In this application this is not a significant drawback, because only the change in the concentration is relevant. The functional principle can be summarized as follows: The air is driven by an integrated fan via the short hose into the device. There it passes a sensor disc which emits photons proportional to the ozone concentration (chemiluminescence). The photons reach a photomultiplier and the output voltage is measured. The functional principle and the measurement theory are explained in detail in (Zahn et al., 2012).

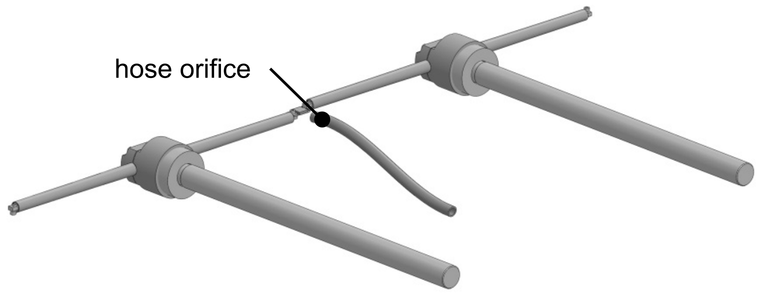

***Figure 10**: 3D drawing of the rotors (without motors) and the location of the hose opening for the ozone measurement*

4.2 Experimental Results

The experiments were carried out in summer, which led to a well sufficient amount of natural ambient ozone. **Fig. 11** shows the raw measurement data from a typical experiment at the test rig. The data acquisition frequency was 25 Hz. The temporal axis starts earlier to achieve a stationary state of the measurement.

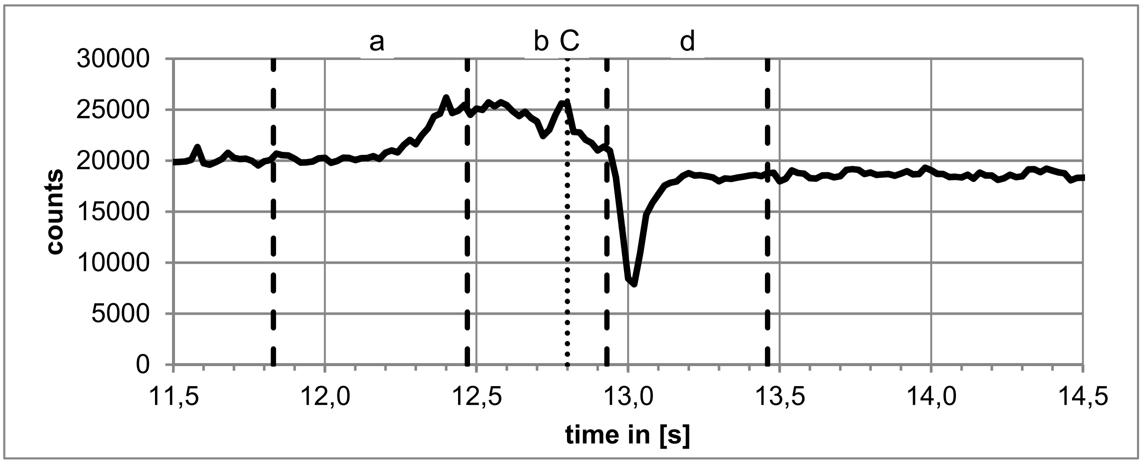

***Figure 11**: Counts over time for a collision experiment at the test rig. The stages of the movement are marked as follows: acceleration (a), constant speed (b), moment of impact (C), deceleration (d).*

When the rotors start after about 11.8 s, the ozone concentration seems to increase shortly afterwards from about 20000 to about 25000 counts for about 0.6 s. This is exactly the time for the acceleration of the rotors, i.e. it takes from the start until the collision takes place. The ozone concentration is delayed by about 0.2 s due to the length of the hose that the air has to travel. When the collision between the specimens takes place after about 12.8 s the ozone concentration drops rapidly to less than 10000 counts. After this drop, the concentration immediately reaches about 18500 counts and thus almost the initial value of 20000 counts. So far, an explanation has not been found for this deviation of about 1500 counts.

4.3 Interpretation

The rise of the concentration within the first second is caused by an aerodynamic effect: The specimens pass the orifice of the suction hose very closely and thus influence the airflow due to air vortices in their vicinity caused by the fast movement of up to 131 m/s. The significant drop of the ozone concentration during the collision indicates that the temperature reaches considerable values. The increased heat leads to excessive ozone decay. Even though absolute values of the ozone concentration cannot be given it appears legitimate to assume temperatures well above 1000 K, which has been proposed by Koschlig et al. (2008). After the impact, the welded parts of the specimens are torn off the rotors. Thus there is no elevated number of counts due to aerodynamic effects at the end, because no sheet specimen passes the orifice of the hose. The rotors are still turning for another 0.5 s until they stop completely. If the test rig's rotors turn with attached specimens, but without any impact, a rise during the acceleration and deceleration can be observed but no drop. The drop can also be found in the data from electromagnetic pulse welding experiments, but here the plateau is not present during the first second before the impact, as was to be expected. **Fig. 12** shows the typical raw measurement data during the weld of two aluminium sheets. The machine setup and the specimens are identical to the vacuum experiments described in chapter 3. The air for measuring the ozone concentration is taken directly next to the impact area of the specimens. Note that the initial ozone concentration is lower and thus the noise seems increased. Also note that the scale of the time axis is different, because the concentration drop lasts longer. This is very likely to be caused by the larger size of the impact area and the higher energy provided by the electromagnetic welding setup compared to the test rig.

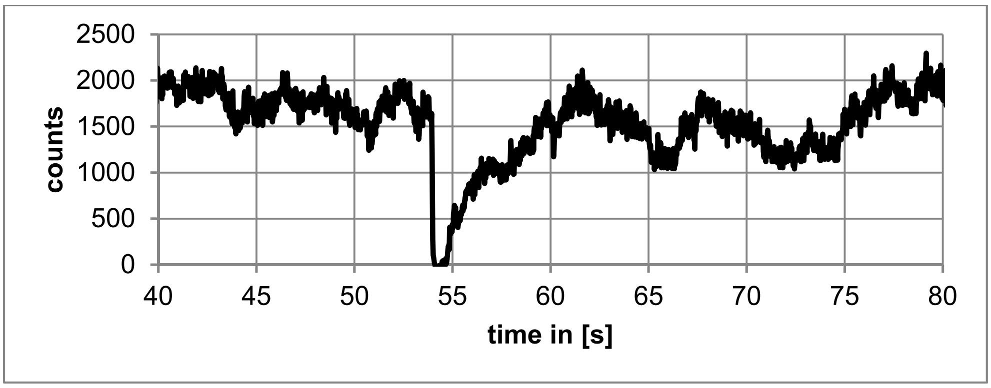

***Figure 12**: Counts over time for electromagnetic pulse welding of two aluminium sheets*

5 Summary and Conclusions

The evaluation of the experimental results shows that the ambient atmosphere has a great impact on the quality of the weld, at least at the lower end of the process window. One possible reason is the air resistance that is experienced by the so-called jet. This theory is supported by the micrographs which show particles in the joint area under normal pressure, but no particles can be observed in the vacuum specimens. In literature, it is generally agreed that jetting is crucial for the formation of the bond. The results also show that the process light is independent from the formation of a jet. The advantage of welding in vacuum decreases with increasing impact energies. However, higher energies are known to lead to an increased formation of intermetallic phases that can reduce the strength of the weld. Thus it can be helpful in some applications to evacuate the space between the workpieces. A significant rise in temperature could be proved by ozone measurements. The excessive decay of ozone during the impact can be explained with a highly elevated temperature in the area between the colliding specimens. However, a possible thermal influence of the plasma on the workpieces' surface cannot be quantified by this method.

6 Outlook on Future Works

To gain more information on the influence of the surrounding gas more experiments will be conducted with different gases and pressures. It will be also investigated if welds of other material combinations can be improved likewise. Equal attention will be paid on the jetting phenomenon, which is expected to have a great influence on the formation of the joint. High speed imaging will be used to investigate the evolution of the jet. Furthermore, a possible influence of an elevated temperature during the impact due to the incurrence of plasma will be investigated. The gas parameters, i.e. pressure and type, will be chosen carefully in order to distinguish the effects on jet formation and temperature evolution.

Acknowledgments

The authors would like to thank the German Research Foundation (DFG) for the financial support of the project GR 1818/49 which enabled this paper. Furthermore, the authors thank Baumüller, PCO AG, Acal BFi and PSTproducts for their support during the experimental works. Further thanks go to Boris Schneider from enviscope GmbH and Andreas Zahn from KIT for supporting the ozone measurements.

References

Bergmann, O. R., Cowan, G. R., Holtzman, A. H., 1966. Experimental Evidence of Jet Formation During Explosion Cladding. In: Transactions of the Metallurgical Society of AIME, Vol. 236, pp. 646-653

Carl, L. R., 1944. Brass welds, made by detonation impulse. In: Metal progress, Vol. 46, pp. 102.

Carpenter, S.H., Wittman, R.H., 1975. Explosion Welding. In: Annu. Rev. Mater. Sci., Vol. 5, pp. 177-199

Clement, J. K., 1904. Über die Bildung des Ozons bei hoher Temperatur. In: Annalen der Physik, Vol. 319, pp. 334-353

Crossland, B., 1982. Explosive welding of metals and its application. In: Oxford series on advanced manufacturing, Oxford University Press, Oxford

Göbel, G., Kaspar, J., Herrmannsdörfer, T., Brenner, B., Beyer, E., 2010. Insights into intermetallic phases on pulse welded dissimilar metal joints. In: 4th International Conference on High Speed Forming, pp. 127-136

Groche, P., Wagner, M. F.-X., Pabst, C., Sharafiev, S., 2014. Development of a novel test rig to investigate the fundamentals of impact welding. In: Journal of Materials Processing Technology, Vol. 214, pp. 2009-2017

Groche, P., Pabst, C., 2015. Numerical Simulation of Impact Welding Processes with LS-DYNA. In: 10th European LS-DYNA Conference

Kakizaki, S., Watanabe, M., Kumai, S., 2011. Simulation and Experimental Analysis of Metal Jet Emission and Weld Interface Morphology in Impact Welding. In: Materials Transactions, Vol. 52, pp. 1003-1008

Kore, S. D., Date, P. P., Kulkarni, S. V., 2007. Effect of process parameters on electromagnetic impact welding of aluminum sheets. In: International Journal of Impact Engineering. Vol. 34, pp. 1327-1341

Koschlig, M., Veehmayer, M., Raabe, D., 2008. Production of Steel-Light Metal Compounds with Explosive Metal Cladding. In: 3rd International Conference on High Speed Forming, pp. 23-32

Pabst, C., Groche, P., 2014. Electromagnetic Pulse Welding: Process Insights by High Speed Imaging and Numerical Simulation. In: 6th International Conference on High Speed Forming, pp. 77-88

Schäfer, R., Pasquale, P., Elsen, A., 2011. Material hybrid joining of sheet metals by electromagnetic pulse technology. In: Key Engineering Materials, Vol. 473, pp. 61-68

Stern, A., Shribman, V., Ben-Artzy, A., Aizenshtein, M., 2014. Interface Phenomena and Bonding Mechanism in Magnetic Pulse Welding. In: Journal of Materials Engineering and Performance, Vol. 23, pp. 3449-3458

Turgutlu, A., Al-Hassani, S. T. S., Akyurt, M., 1995. Experimental investigation of deformation and jetting during impact spot welding. In: International Journal of Impact Engineering, Vol. 16, pp. 789-799

Wang, X., Zheng, Y., Liu, H., Shen, Z., Hu, Y., Li, W., Gao, Y., Guo, C., 2012. Numerical study of the mechanism of explosive/impact welding using Smoothed Particle Hydrodynamics method. In: Materials and Design, Vol. 35, pp. 210-219

Watanabe, M., Kumai, S., 2009. High-Speed Deformation and Collision Behavior of Pure Aluminum Plates in Magnetic Pulse Welding. In: Materials Transactions, Vol. 50, pp. 2035-2042

Zahn, A., Weppner, J., Widmann, H., Schlote-Holubek, K., Burger, B., Kühner, T., Franke, H., 2012. A fast and precise chemiluminescence ozone detector for eddy flux and airborne application. In: Atmospheric Measurement Techniques, Vol. 5, pp. 363–375